Outage Probability Analysis of Cognitive Decode-and-Forward Relay Networks over $\kappa-\mu$ Shadowed Channels

Sikandar Kumar and Sonali Chouhan,
Department of Electronics and Electrical Engineering
Indian Institute of Technology, Guwahati
Assam, 781039, India
Email: {k.sikandar, sonali}@iitg.ernet.in

***Abstract*—A primary and cognitive relay spectrum sharing network is considered. The channels are assumed to be $\kappa-\mu$ shadowed fading with arbitrary fading parameters. We obtained expression for outage probability to analyze the performance under the power constraints on maximum transmit power at secondary user (SU) transmitter and relay, and peak interference power at primary user (PU) receiver. The performance of the cognitive relay network is analyzed for various fading parameters and power constraints, which are validated by Monte-Carlo simulations. It is shown that an outage floor is reached when peak interference power at PU receiver is independent of transmitting power at SU transmitter and relay, which gives insight to design a cognitive relay network in the presence of PU network.**

***Index Terms*—Cognitive radio, $\kappa-\mu$ shadowed channel, Hypergeometric function, Outage probability.**

I. Introduction

Spectrum sharing (SS) network in the context of cognitive radio (CR), where the secondary users (SU) share same spectrum allocated to the primary users (PU), is capable to solve spectrum scarcity issues, thereby to increase the available spectrum utilization [1]. The performance of SU is limited by maximum transmit power constraint at SU transmitter (SU-Tx) to satisfy the peak interference power at the PU receiver (PU-Rx). Further intermediate relays in CR network are exploited to overcome deeply faded channel between SU-Tx and SU receiver (SU-Rx) and also to expand the coverage of SU nodes [2]. Most of the works in the literature have been analyzed under Rayleigh or Nakagami faded channels [3]–[8]. In order to improve the performance and the quality of service of the CR networks, it needs to be analyzed under realistic channel models. Recently, $\kappa-\mu$ shadowed channel fading has been proposed [9] which is the generalization of $\kappa-\mu$ fading [10] and Rician shadowed fading [11]. The proposed channel model is more realistic to describe the cognitive relay networks than Rayleigh or Nakagami faded channel models [12]. To the best of our knowledge, no work has been reported in open literature which analyzes the SS network in the context of CR with power constraints under $\kappa-\mu$ shadowed channel.

In this paper, a primary and cognitive relay spectrum sharing network is considered. The cognitive relay network comprises a SU-Tx, a decode-and-forward (DF) relay (SU-R), and a SU-Rx. Single PU-Rx node is considered at primary side which exists within the coverage area of SU nodes. The transmitting power at the SU-Tx and SU-R are constrained by peak interference power at PU-Rx. All channels are assumed to be $\kappa-\mu$ shadowed fading with arbitrary fading parameters. The approximate and asymptotic outage probabilities (OP) are obtained to analyze the performance of the cognitive relay network. The outage analysis for various fading parameters under power constraints at SU-Tx and SU-R gives insight to design a cognitive relay network in the presence of PU network.

The remaining paper is organized as follows: system and channel models are described in Section II. Expressions for approximate and asymptotic OP are obtained in Section III. Simulation results are discussed in Section IV, and finally conclusions are deduced in Section V.

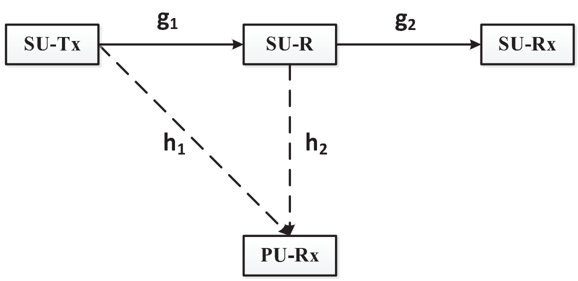

Fig. 1. A two hop cognitive decode-and-forward relay network in coexistence with a primary user receiver.

II. System and Channel Models

A. System Model

A two hop cognitive relay network consists of a SU-Tx, a DF SU-R, and a SU-Rx which shares the same spectrum allotted to the PU network. A single PU-Rx is considered which exists within the coverage area of SU nodes. Each node consists of a single antenna. This simplified scenario is considered for the ease of analysis which is shown in Fig. 1. The communication at a two hop CR relay network is completed in two distinct time slots. In first time slot, the SU-Tx transmits the signal to SU-R, and in second time slot, the SU-R node decodes the received signal and forwards it to the SU-Rx. The maximum allowable transmitted power at SU-Tx and SU-R are denoted by P, which is constrained by the peak interference power at PU-Rx denoted by I. Thus, the transmitted power at SU-Tx and SU-R are denoted by P_S and P_R, respectively, and are constrained as

$$P_S = \min\left(P, \frac{I}{|h_1|^2}\right), \quad P_R = \min\left(P, \frac{I}{|h_2|^2}\right) \tag{1}$$

where h_1 and h_2 are the channel fading coefficients of links between SU-Tx to PU-Rx and SU-R to PU-Rx, respectively. The instantaneous signal-to-noise ratio (SNR) at SU-R and SU-Rx are denoted by γ_R and γ_D, respectively, and are given by

$$\gamma_R = \frac{P_S |g_1|^2}{N_0}, \quad \gamma_D = \frac{P_R |g_2|^2}{N_0} \tag{2}$$

where g_1 and g_2 are the channel fading coefficients of links between SU-Tx to SU-R and SU-R to SR-Rx, respectively. N_0 is the noise power of additive white Gaussian noise (AWGN). From (1) and (2), we get

$$\gamma_R = \min\left(\gamma_P |g_1|^2, \frac{\gamma_I |g_1|^2}{|h_1|^2}\right) \tag{3}$$

$$\gamma_D = \min\left(\gamma_P |g_2|^2, \frac{\gamma_I |g_2|^2}{|h_2|^2}\right) \tag{4}$$

where $\gamma_P = \frac{P}{N_0}$ and $\gamma_I = \frac{I}{N_0}$. The end-to-end instantaneous SNR at SU-Rx is $\gamma = \min(\gamma_R, \gamma_D)$.

B. Channel Model

The power of instantaneous channel coefficients are assumed to be $\kappa - \mu$ shadowed fading with arbitrary fading parameters, i.e., $\left\{|g_i|^2, |h_i|^2\right\} \sim S_{\kappa\mu}(\kappa_i, \mu_i, m_i; \bar{\gamma}_i)$ where $(\kappa_1, \mu_1, m_1; \bar{\gamma}_1)$, $(\kappa_2, \mu_2, m_2; \bar{\gamma}_2)$, $(\kappa_3, \mu_3, m_3; \bar{\gamma}_3)$, and $(\kappa_4, \mu_4, m_4; \bar{\gamma}_4)$ are fading parameters of SU-Tx $\rightarrow$ SU-R, SU-R $\rightarrow$ SU-Rx, SU-Tx $\rightarrow$ PU-Rx, and SU-R $\rightarrow$ PU-Rx, respectively. $\bar{\gamma}_i$ is the average power of channel fading of respective links. The probability density function (PDF) of $\kappa - \mu$ shadowed fading is given by [9]

$$f_Z(z) = \frac{\phi_1^{m-\mu} z^{\mu-1}}{\phi_2^m \Gamma(\mu)} e^{-\frac{z}{\phi_1}} {}_1F_1\left(m; \mu; \frac{(\phi_2 - \phi_1) z}{\phi_1 \phi_2}\right) \tag{5}$$

where $\phi_1 = \frac{\bar{\gamma}}{\mu(1+\kappa)}$, $\phi_2 = \frac{(\mu\kappa+m)\bar{\gamma}}{\mu(1+\kappa)m}$, and ${}_1F_1$ is the Kummer confluent hypergeometric function. We approximate the $\kappa - \mu$ shadowed random variable (RV) by gamma RV denoted by $\mathcal{G}(\alpha_i, \beta_i)$ as in [13], where

$$\alpha_i = \frac{m_i \mu_i (1+\kappa_i)^2}{m_i + \mu_i \kappa_i^2 + 2 m_i \kappa_i}, \quad \beta_i = \frac{\bar{\gamma}_i}{\alpha_i}. \tag{6}$$

Here, $\{\alpha_i, \beta_i\}, i \in \{1,2,3,4\}$ are the gamma variates of links between SU-Tx $\rightarrow$ SU-R, SU-R $\rightarrow$ SU-Rx, SU-Tx $\rightarrow$ PU-Rx, and SU-R $\rightarrow$ PU-Rx, respectively. The cumulative distribution function (CDF) of power of instantaneous channel coefficients are given by [13]

$$F_Z(z) = \frac{z^{\alpha_i}}{\beta_i^{\alpha_i} \Gamma(\alpha_i + 1)} {}_1F_1\left(\alpha_i; \alpha_i + 1; \frac{-z}{\beta_i}\right). \tag{7}$$

III. Outage Probability

In this section, we derive approximate and asymptotic OP for two hop CR DF relay network, which is mathematically defined as [3]

$$\begin{aligned} P_{out} &= \Pr\{\min(\gamma_R, \gamma_D) \leqslant \gamma_{th}\} \\ &= F_{\gamma_R}(\gamma_{th}) + F_{\gamma_D}(\gamma_{th}) - F_{\gamma_R}(\gamma_{th}) F_{\gamma_D}(\gamma_{th}) \end{aligned} \tag{8}$$

where $F_{\gamma_R}(\cdot)$ and $F_{\gamma_D}(\cdot)$ are the CDFs of instantaneous SNRs at SU-R and SU-Rx, respectively, that we derive in the next subsection using (3) and (4). γ_{th} denotes the outage threshold.

A. Approximate Analysis

The CDF of instantaneous SNR at SU-R can be derived as

$$\begin{aligned} F_{\gamma_R}(\gamma_{th}) &= \Pr(\gamma_R \leqslant \gamma_{th}) \\ &= \Pr\left(|g_1|^2 \leqslant \frac{\gamma_{th}}{\gamma_P}, |h_1|^2 \leqslant \frac{\gamma_I}{\gamma_P}\right) \\ &+ \Pr\left(\frac{|g_1|^2}{|h_1|^2} \leqslant \frac{\gamma_{th}}{\gamma_I}, |h_1|^2 \geqslant \frac{\gamma_I}{\gamma_P}\right) \\ &= \Im_1 + \Im_2. \end{aligned} \tag{9}$$

Using (7), first part $\Im_1$ in (9) is obtained as

$$\begin{aligned} \Im_1 &= F_{|g_1|^2}\left(\frac{\gamma_{th}}{\gamma_P}\right) F_{|h_1|^2}\left(\frac{\gamma_I}{\gamma_P}\right) \\ &= \frac{\gamma_{th}^{\alpha_1} \gamma_I^{\alpha_3}}{\gamma_P^{\alpha_1+\alpha_3} \beta_1^{\alpha_1} \beta_3^{\alpha_3} \Gamma(\alpha_1+1) \Gamma(\alpha_3+1)} \\ &\quad {}_1F_1\left(\alpha_1; \alpha_1+1; \frac{-\gamma_{th}}{\gamma_P \beta_1}\right) {}_1F_1\left(\alpha_3; \alpha_3+1; \frac{-\gamma_I}{\gamma_P \beta_3}\right). \end{aligned} \tag{10}$$

The second part $\Im_2$ in (9) can be obtained as

$$\Im_2 = \int_{\frac{\gamma_I}{\gamma_P}}^{\infty} F_{|g_1|^2}\left(\frac{\gamma_{th} y}{\gamma_I}\right) f_{|h_1|^2}(y)\, dy \tag{11}$$

where $f_{|h_1|^2}(y)$ is the PDF of $|h_1|^2$ which is given by

$$f_{|h_1|^2}(y) = \frac{y^{\alpha_3-1} e^{\frac{-y}{\beta_3}}}{\beta_3^{\alpha_3} \Gamma(\alpha_3)}. \tag{12}$$

Using (7) and (12), (11) can be written as

$$\begin{aligned} \Im_2 = &\frac{\gamma_{th}^{\alpha_1}}{\gamma_I^{\alpha_1} \beta_1^{\alpha_1} \beta_3^{\alpha_3} \Gamma(\alpha_1+1) \Gamma(\alpha_3)} \\ &\int_{\frac{\gamma_I}{\gamma_P}}^{\infty} y^{\alpha_1+\alpha_3-1} e^{\frac{-y}{\beta_3}} {}_1F_1\left(\alpha_1; \alpha_1+1; \frac{-\gamma_{th} y}{\gamma_I \beta_1}\right) dy. \end{aligned} \tag{13}$$

Using the transformation ${}_1F_1(a;b;-z) = e^{-z}{}_1F_1(b-a;b;z)$ given in [14], (13) can be written as

$$\Im_2 = C_1 \int_{\frac{\gamma_I}{\gamma_P}}^{\infty} y^{\alpha_1+\alpha_3-1} e^{-y\left(\frac{1}{\beta_3}+\frac{\gamma_{th}}{\gamma_I\beta_1}\right)} {}_1F_1\left(1;\alpha_1+1;\frac{\gamma_{th}y}{\gamma_I\beta_1}\right) dy \quad (14)$$

where $C_1 = \frac{\gamma_{th}^{\alpha_1}}{\gamma_I^{\alpha_1}\beta_1^{\alpha_1}\beta_3^{\alpha_3}\Gamma(\alpha_1+1)\Gamma(\alpha_3)}$. The integration involved in (14) is mathematically intractable. We use series representation of ${}_1F_1$ [15, eq. (9.14.1)], thus (14) can be written as

$$\Im_2 = C_1 \int_{\frac{\gamma_I}{\gamma_P}}^{\infty} \sum_{n=0}^{\infty} \frac{\Gamma(\alpha_1+1)\gamma_{th}^n}{\Gamma(\alpha_1+n+1)\gamma_I^n\beta_1^n} y^{\alpha_1+\alpha_3+n-1} e^{-y\left(\frac{1}{\beta_3}+\frac{\gamma_{th}}{\gamma_I\beta_1}\right)} dy. \quad (15)$$

The sequence involved in (15) is unsigned and non-negative. Hence, using Tonelli's theorem [16, Corollary 1.4.46], the integration and summation can be interchanged in (15), and is written as

$$\Im_2 = C_1 \sum_{n=0}^{\infty} \frac{\Gamma(\alpha_1+1)\gamma_{th}^n}{\Gamma(\alpha_1+n+1)\gamma_I^n\beta_1^n} \int_{\frac{\gamma_I}{\gamma_P}}^{\infty} y^{\alpha_1+\alpha_3+n-1} e^{-y\left(\frac{1}{\beta_3}+\frac{\gamma_{th}}{\gamma_I\beta_1}\right)} dy. \quad (16)$$

The integration involved in (16) is solved using [15, eq. (3.351.2)] to obtain

$$\Im_2 = C_3 \sum_{n=0}^{\infty} \frac{C_2^n\beta_3^n\Gamma\left(\alpha_1+\alpha_3+n, \frac{\gamma_I}{\gamma_P\beta_3}(1+C_2\beta_3)\right)}{(1+C_2\beta_3)^n\Gamma(\alpha_1+n+1)} \quad (17)$$

where $C_2 = \frac{\gamma_{th}}{\gamma_I\beta_1}$ and $C_3 = \frac{(C_2\beta_3)^{\alpha_1}}{(1+C_2\beta_3)^{\alpha_1+\alpha_3}\Gamma(\alpha_3)}$. Hence, the CDF of instantaneous SNR at SU-R $F_{\gamma_R}(\gamma_{th})$ is obtained by adding (10) and (17) as in (9), and finally given in (24). Similarly, the CDF of instantaneous SNR at SU-Rx $F_{\gamma_D}(\gamma_{th})$ is obtained by replacing $\alpha_1 \to \alpha_2$, $\beta_1 \to \beta_2$, $\alpha_3 \to \alpha_4$, $\beta_3 \to \beta_4$ in (24). Using CDFs of γ_R and γ_D, the OP can be obtained easily according to (8).

The series involved in CDF expressions as in (24) can be truncated to N finite terms such that $\varepsilon_N < 10^{-3}$, with

$$\varepsilon_N = F_{\gamma_{R,N}} - F_{\gamma_{R,N-1}} = \frac{C_3\Gamma\left(\alpha_1+\alpha_3+N, \frac{\gamma_I}{\gamma_P\beta_3}(1+C_2\beta_3)\right)}{\left(1+\frac{1}{C_2\beta_3}\right)^N\Gamma(\alpha_1+N+1)} \quad (18)$$

where $F_{\gamma_{R,N}}$ and $F_{\gamma_{R,N-1}}$ denote the CDFs truncated to N and $N-1$ finite terms, respectively. Denominator in (18) consists of power and factorial in N whereas numerator consists of incomplete gamma function involving N. Hence, as N increases the denominator increases faster than the numerator, and $\varepsilon_N \to 0$.

B. Asymptotic Analysis

In this section, we consider that the peak interference power at PU-Rx from SU-Tx and SU-R are fixed to I. However, the transmitting power at SU-Tx and SU-R nodes are increasing in high SNR region. The maximum transmitting power at SU-Tx and SU-R are constrained by I as modeled in (1), and the asymptotic OP can be obtained as

$$P_{out}^{\infty} \approx F_{\gamma_R}^{\infty}(\gamma_{th}) + F_{\gamma_D}^{\infty}(\gamma_{th}) - F_{\gamma_R}^{\infty}(\gamma_{th}) F_{\gamma_D}^{\infty}(\gamma_{th}). \quad (19)$$

The asymptotic CDF of instantaneous SNR at SU-R is calculated as

$$F_{\gamma_R}^{\infty} \approx \Im_1^{\infty} + \Im_2^{\infty}. \quad (20)$$

$\Im_1^{\infty}$ can be obtained after simplifying $\Im_1$ in (10), using the power series expansion of ${}_1F_1$ as $z \to 0$, which is given by [17]

$${}_1F_1(a;b;z) = 1 + \frac{az}{b} + \frac{a(1+a)z^2}{2b(1+b)} + O\left(z^3\right). \quad (21)$$

To solve for $\Im_2^{\infty}$ from (11), we apply transformation of variable $y = \frac{\gamma_I}{\gamma_P}x$ and can be written as

$$\Im_2 = \int_1^{\infty} \frac{\gamma_I}{\gamma_P} F_{|g_1|^2}\left(\frac{\gamma_{th}x}{\gamma_P}\right) f_{|h_1|^2}\left(\frac{\gamma_I}{\gamma_P}x\right) dx. \quad (22)$$

The expression obtained for $\Im_2^{\infty}$ is same as given in (17). To alleviate the computational complexity, only first term is considered which corresponds to $n = 0$ in (17). Thus, $\Im_2^{\infty}$ is obtained as

$$\Im_2^{\infty} \approx \frac{C_3\Gamma\left(\alpha_1+\alpha_3, \frac{\gamma_I(1+C_2\beta_3)}{\gamma_P\beta_3}\right)}{\Gamma(\alpha_1+1)}. \quad (23)$$

Hence, $F_{\gamma_R}^{\infty}$ in (20) can be calculated from (10), (21) and (23), and finally given in (25). Similarly, the asymptotic CDF of instantaneous SNR at SU-Rx $F_{\gamma_D}^{\infty}$ can be determined by replacing $\alpha_1 \to \alpha_2$, $\beta_1 \to \beta_2$, $\alpha_3 \to \alpha_4$, $\beta_3 \to \beta_4$ in (25). Finally, the asymptotic OP can be obtained easily using $F_{\gamma_R}^{\infty}$ and $F_{\gamma_D}^{\infty}$ as described in (19).

IV. Simulation Results

In this section, the considered two hop cognitive DF relay network with peak interference power at PU-Rx is simulated for various values of parameters. Single SU-Tx, DF relay, SU-Rx and PU-Rx are considered with single antenna at each node. The effect of relative distances between nodes can be incorporated by the values of fading parameters defined in (6). The average power of channel fading $\bar{\gamma}_i$ is normalized to unity for each link between nodes. The noise power at SU-R and SU-Rx nodes are also normalized to unity. The outage threshold γ_{th} is set to 0 dB. To compute series involved in CDF and OP expressions, we take $N = 21$ so that $\varepsilon_N < 10^{-3}$ as calculated from (18). Each simulation is averaged over 10^6 independent realizations.

$$F_{\gamma_R}\left(\gamma_{th}\right) = \frac{\gamma_{th}^{\alpha_1}\gamma_I^{\alpha_3}}{\gamma_P^{\alpha_1+\alpha_3}\beta_1^{\alpha_1}\beta_3^{\alpha_3}\Gamma\left(\alpha_3\right)}\left[\frac{1}{\alpha_3\Gamma\left(\alpha_1+1\right)}{}_1F_1\left(\alpha_1;\alpha_1+1;\frac{-\gamma_{th}}{\gamma_P\beta_1}\right){}_1F_1\left(\alpha_3;\alpha_3+1;\frac{-\gamma_I}{\gamma_P\beta_3}\right)+\left(\frac{\gamma_P\beta_1\beta_3}{\gamma_I\beta_1+\gamma_{th}\beta_3}\right)^{\alpha_1+\alpha_3}\sum_{n=0}^{\infty}\frac{1}{\Gamma\left(\alpha_1+n+1\right)}\left(1+\frac{\gamma_I\beta_1}{\gamma_{th}\beta_3}\right)^{-n}\Gamma\left(\alpha_1+\alpha_3+n,\frac{\gamma_I\beta_1+\gamma_{th}\beta_3}{\gamma_P\beta_1\beta_3}\right)\right]. \quad (24)$$

$$F_{\gamma_R}^{\infty}\left(\gamma_{th}\right) \approx \frac{\gamma_{th}^{\alpha_1}\gamma_I^{\alpha_3}}{\gamma_P^{\alpha_1+\alpha_3}\beta_1^{\alpha_1}\beta_3^{\alpha_3}\Gamma\left(\alpha_1+1\right)\Gamma\left(\alpha_3\right)}\left[\frac{1}{\alpha_3}\left(1-\frac{\alpha_1}{\left(\alpha_1+1\right)}\frac{\gamma_{th}}{\gamma_P\beta_1}+\frac{\alpha_1}{2\left(\alpha_1+2\right)}\left(\frac{\gamma_{th}}{\gamma_P\beta_1}\right)^2\right)\times\left(1-\frac{\alpha_3}{\left(\alpha_3+1\right)}\frac{\gamma_I}{\gamma_P\beta_3}+\frac{\alpha_3}{2\left(\alpha_3+2\right)}\left(\frac{\gamma_I}{\gamma_P\beta_3}\right)^2\right)+\left(\frac{\gamma_P\beta_1\beta_3}{\gamma_I\beta_1+\gamma_{th}\beta_3}\right)^{\alpha_1+\alpha_3}\Gamma\left(\alpha_1+\alpha_3,\frac{\gamma_I\beta_1+\gamma_{th}\beta_3}{\gamma_P\beta_1\beta_3}\right)\right]. \quad (25)$$

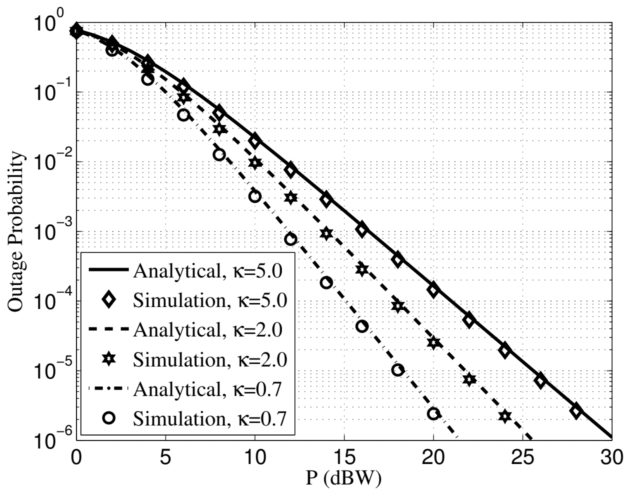

Fig. 2. OP versus transmit power at SU nodes for different values of $\{\kappa_i,\mu_i,m_i\}_{i=1}^4 = \{\{\kappa,3.5,2\},\{\kappa,5.0,1.7\},\{\kappa,2.5,0.7\},\{\kappa,3.0,2.2\}\}$ and $I = 2P$.

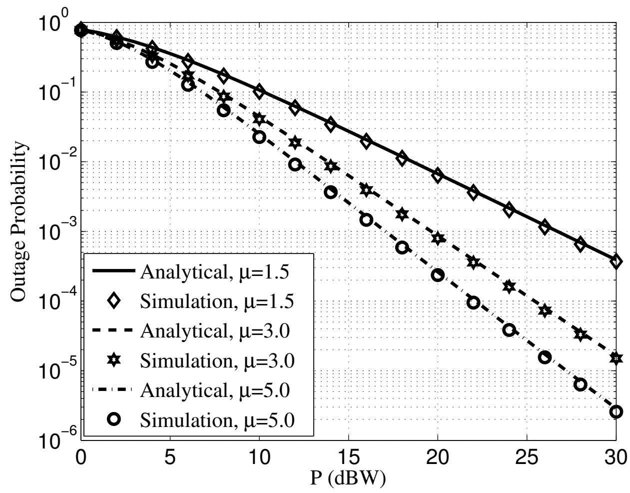

Fig. 4. OP versus transmit power at SU nodes for different values of μ when $\{\kappa_i,\mu_i,m_i\}_{i=1}^4 = \{\{0.5,\mu,0.5\},\{1.7,\mu,1.0\},\{2.4,\mu,1.1\},\{0.7,\mu,0.7\}\}$ and $I = 2P$.

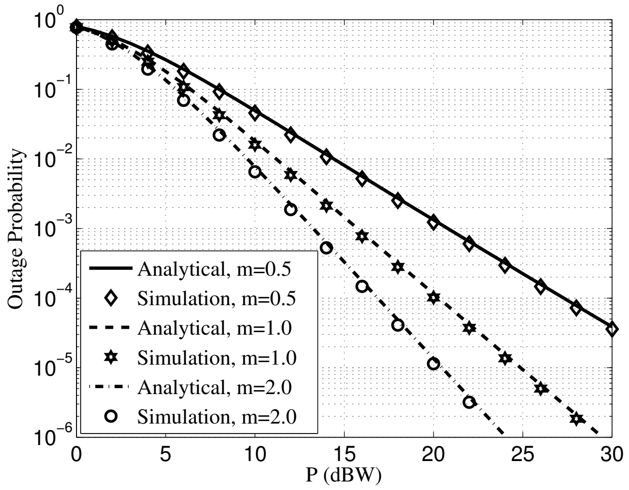

Fig. 3. OP versus transmit power at SU nodes for different values of m when $\{\kappa_i,\mu_i,m_i\}_{i=1}^4 = \{\{0.5,3.5,m\},\{0.8,3.0,m\},\{0.4,4.5,m\},\{0.7,5.7,m\}\}$ and $I = 2P$.

Figures 2-4 show the OP for different values of fading parameters κ, m, and μ, respectively, for the fixed values of $\{\mu_i,m_i\}$, $\{\kappa_i,\mu_i\}$, and $\{\kappa_i,m_i\}$, respectively, for particular links. The OPs are shown for different values of transmitted power P at SU nodes when peak interference power I at PU-Rx is assumed to be twice of P. It is seen that the OP improves continuously without outage floor as P improves. It is also observed that the OP degrades as the value of κ increases (shown in Fig. 2), however it improves as the values of m and/or μ increase (shown in Fig. 3 and Fig. 4, respectively) simultaneously between links at all four nodes. This analysis can easily be extended by varying the fading parameters of a single link while keeping them fixed for rest of the links.

In Fig. 5, the system performance is shown for various values of P when I is fixed and predefined to 9 dBW, 15 dBW, and 18 dBW. In this scenario, as P increases the transmitted power at SU nodes P_S and P_R restricted by I. Initially, when the value of P increases the OP decreases up to a point, determined by the value of I. Beyond this point, on increasing the value of P, the OP approaches an outage floor. Hence, it

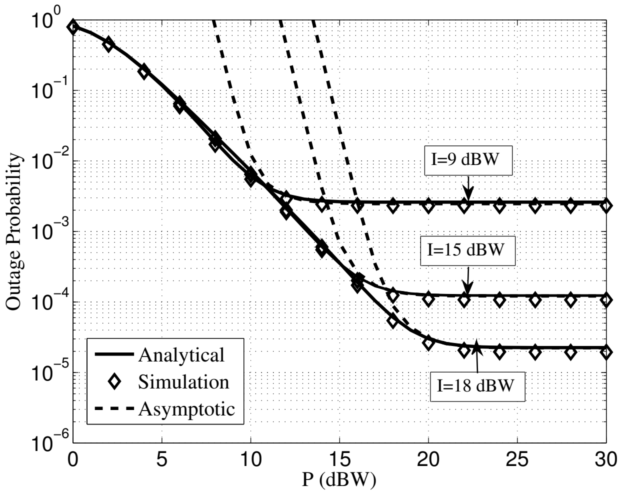

Fig. 5. OP versus transmit power at SU nodes with different values of peak interference power I when $\{\kappa_i, \mu_i, m_i\}_{i=1}^{4} = \{\{0.5, 4.5, 3\}, \{0.8, 3.0, 1.7\}, \{0.4, 4.7, 2.2\}, \{0.7, 1.7, 1.0\}\}$.

gives insight that in a primary and secondary shared network, the SU nodes can transmit with transmit power within a limit such that the interference limit at the PU-Rx is maintained.

Extensive simulations are performed for various fading parameters and power constraints. For brevity, a subset of them are presented here. Simulation results are shown to be closely matched with analytical results which validate our derivations.

V. Conclusions

A two hop cognitive DF relay network is considered which share spectrum allotted to the primary network under constrained transmit power at SU nodes. The approximate and asymptotic outage probabilities are calculated in $\kappa - \mu$ shadowed channels with arbitrary fading parameters. It is shown that the outage probability improves continuously when peak interference power at PU-Rx is proportional to the transmit power at SU nodes. However, an outage floor is approached when peak interference power at PU-Rx is predefined to a fixed value which is independent of the transmit power of SU nodes. The observations reported in this paper provided useful insight to the cognitive network designer about the system performance in realistic channel environment.

References

[1] A. Goldsmith, S. Jafar, I. Maric, and S. Srinivasa, "Breaking spectrum gridlock with cognitive radios: An information theoretic perspective," *Proceedings of the IEEE*, vol. 97, no. 5, pp. 894–914, May 2009.

[2] Y. Guo, G. Kang, N. Zhang, W. Zhou, and P. Zhang, "Outage performance of relay-assisted cognitive-radio system under spectrum-sharing constraints," *Electronics Letters*, vol. 46, no. 2, pp. 182–184, Jan. 2010.

[3] T. Duong, P. L. Yeoh, V. N. Q. Bao, M. Elkashlan, and N. Yang, "Cognitive relay networks with multiple primary transceivers under spectrum-sharing," *IEEE Signal Processing Letters*, vol. 19, no. 11, pp. 741–744, Nov. 2012.

[4] X. Zhang, Y. Zhang, Z. Yan, J. Xing, and W. Wang, "Performance analysis of cognitive relay networks over Nakagami- m fading channels," *IEEE Journal on Selected Areas in Communications*, vol. 33, no. 5, pp. 865–877, May 2015.

[5] F. Khan, K. Tourki, M.-S. Alouini, and K. Qaraqe, "Performance analysis of a power limited spectrum sharing system with TAS/MRC," *IEEE Transactions on Signal Processing*, vol. 62, no. 4, pp. 954–967, Feb. 2014.

[6] P. Yeoh, M. Elkashlan, K. Kim, T. Duong, and G. Karagiannidis, "Transmit antenna selection in cognitive MIMO relaying with multiple primary transceivers," *IEEE Transactions on Vehicular Technology*, vol. PP, no. 99, pp. 1–1, 2015.

[7] Y. Deng, M. Elkashlan, P. L. Yeoh, N. Yang, and R. Mallik, "Cognitive MIMO relay networks with generalized selection combining," *IEEE Transactions on Wireless Communications*, vol. 13, no. 9, pp. 4911–4922, Sep. 2014.

[8] P. L. Yeoh, M. Elkashlan, T. Duong, N. Yang, and D. da Costa, "Transmit antenna selection for interference management in cognitive relay networks," *IEEE Transactions on Vehicular Technology*, vol. 63, no. 7, pp. 3250–3262, Sep. 2014.

[9] J. Paris, "Statistical characterization of $\kappa-\mu$ shadowed fading," *IEEE Transactions on Vehicular Technology*, vol. 63, no. 2, pp. 518–526, Feb. 2014.

[10] M. Yacoub, "The $\kappa - \mu$ distribution and the $\eta - \mu$ distribution," *IEEE Antennas and Propagation Magazine*, vol. 49, no. 1, pp. 68–81, Feb. 2007.

[11] A. Abdi, W. Lau, M.-S. Alouini, and M. Kaveh, "A new simple model for land mobile satellite channels: first- and second-order statistics," *IEEE Transactions on Wireless Communications*, vol. 2, no. 3, pp. 519–528, May 2003.

[12] S. Cotton, "Human body shadowing in cellular device-to-device communications: Channel modeling using the shadowed $\kappa - \mu$ fading model," *IEEE Journal on Selected Areas in Communications*, vol. 33, no. 1, pp. 111–119, Jan. 2015.

[13] S. Kumar, "Approximate outage probability and capacity for $\kappa-\mu$ shadowed fading," *IEEE Wireless Communications Letters*, vol. 4, no. 3, pp. 301–304, Jun. 2015.

[14] L. J. Slater, *Confluent Hypergeometric Functions*. University Press Cambridge, 1960.

[15] I. S. Gradshteyn and I. M. Ryzhik, *Tables of integrals, series and products*, 7th ed., A. Jeffrey and D. Zwillinger, Eds. Elsevier, 2007.

[16] T. Tao, "An introduction to measure theory," American Mathematical Soc. vol. 126, 2011.

[17] [Online]. Available: http://functions.wolfram.com/07.20.06.0016.01